ISSN 2075-1133, Inorganic Materials: Applied Research, 2019, Vol. 10, No. 2, pp. 438–444. © Pleiades Publishing, Ltd., 2019.
Russian Text © S.A. Ghyngazov, V. Kostenko, V.V. Ovchinnikov, N.V. Gushchina, F.F. Makhinko, 2018, published in Perspektivnye Materialy, 2018, No. 8, pp. 61–71.

NEW TECHNOLOGIES OF PREPARATION AND TREATMENT OF MATERIALS

Surface Modification of Corundum Ceramics by Argon Ion Beam

S. A. Ghyngazov[a], *, V. Kostenko[a], V. V. Ovchinnikov[b], **, *, N. V. Gushchina[b], ****, *****, and F. F. Makhinko[b], ********

[a] *National Research Tomsk Polytechnic University, Tomsk, 634050 Russia*

[b] *Institute of Electrophysics, Ural Branch, Russian Academy of Sciences, Yekaterinburg, 620016 Russia*

**e-mail: ghyngazov@tpu.ru*

***e-mail: Vladimir@iep.uran.ru*

****e-mail: viae05@rambler.ru*

*****e-mail: gushchina@iep.uran.ru*

******e-mail: guscha@rambler.ru*

*******e-mail: ffm1978@mail.ru*

Received March 29, 2018; revised May 14, 2018; accepted May 15, 2018

Abstract—The mechanical properties of near-surface layers of aluminum oxide ceramic treated with a continuous ion beam of argon are investigated. The phase and structural changes of the modified near-surface layers were analyzed by X-ray diffraction analysis and scanning electron microscopy, respectively. Samples for research were made from corundum plates used in microelectronics. Ion processing was carried out using an ILM-1 ion implanter equipped with a Pulsar-1M ion source based on a low-pressure glow discharge with a cold hollow cathode. Argon ions with energy of 30 keV and ion current density $j = 300$ μA/cm^2 were used for the irradiation. Two irradiation modes with the fluences of 10^{16} and 10^{17} cm^{-2} were implemented. It was established that the ion treatment promotes the manifestation of the initial grain structure of a sample and increases the mechanical characteristics (modulus of elasticity and nanohardness) of near-surface layers of samples. According to the X-ray diffraction data, after the action of an ion beam, there is a decrease in the size of the coherent scattering region with respect to the initial state. The irradiation leads to an increase in the values of crystal lattice microstrains. Possible mechanisms of modifying the ceramic surface are discussed.

Keywords: aluminum oxide ceramic (corundum), ion beams, mechanical characteristics, X-ray phase analysis

DOI: 10.1134/S2075113319020199

INTRODUCTION

The manufacture of materials for electronics and materials for functional purposes and tools demands structures with gradient properties. The development of such structures makes it possible to effectively change the optical, mechanical, and electric properties of near-surface layers of different materials with respect to volume layers. One of the trends in the development of gradient structures is represented by radiation treatment techniques such as surface treatment with high-current pulsed beams of low-energy electrons [1–4], laser treatment [5, 6], and ion beam treatment [7–18]. Ion beams with the ion energy of 25–50 keV are widely used for the implantation of semiconductors [17–19]. Recently, there appeared new ion accelerators providing ion beams of different ions in a wide range of energies and power densities [20–24], which are used for the modification of metals and alloys [25–31]. Ion beams of different ions (both continuous and pulsed) with energies of several keV to hundreds of keV are used.

It is of interest to use the ion treatment for the modification of ceramic materials. Since they are characterized by increased strength, chemical resistance, and melting point, the ion modification can be used for the development of gradient ceramic structures, which is mostly impossible using the classic treatment techniques. Examples of the use of ion beams for modification near-surface layers of ceramic materials are given in [8, 14–16]. It is shown that the treatment with high-intensity ion beams leads to the change in the phase and chemical composition of near-surface layers and the development of a microstructure with a significantly smaller grain size than in the ceramic volume. Thus, ion beams can be used for the effective modification of near-surface properties of ceramic materials. The issue of the mechanisms of ion impact on the properties of materials is the subject of study of many researchers.

The issue of the mechanisms of ion impact on the properties of materials is widely explored. Apparently, the actualization of possible mechanisms is highly dependent on the type of ions, their energy, the treat-

ment conditions, and the type of material. In [32–34], it is shown that the treatment of metals and alloys with argon ion beams with the energy of about 20–40 keV is accompanied by the modification of their mechanical properties, which is manifested by strengthening of treated tape metal materials much deeper than the depth of ion penetration during the treatment. Owing to the fact that, under such accelerating voltages and current densities, no noticeable surface erosion of treated material occurs, it is of interest from both the scientific and practical viewpoint to establish the regularities of impact of this type of ion treatment on ceramic materials widely used, e.g., in microelectronics.

In microelectronics, corundum ceramic is especially important, being predominantly used as a substrate material. Along with locating active elements on the ceramic surface, current conductive layers are formed, e.g., by thermal or ion-plasma spraying of metal targets in vacuum. Aluminum oxide ceramic has increased hardness, stable phase composition, and high dielectric characteristics. The development of methods for control of structure and properties of this type of ceramic by ion treatment can widen significantly the scope of this type of ceramic. It is important to know how the ion treatment affects its functional properties. In addition, since aluminum oxide ceramic is characterized by an increased hardness and the phase composition stability, this type of ceramic is of interest as a model material for the study of the processes of modification of ceramic and metal materials by ion treatment.

The aim of this work is to study the effect of the surface treatment with continuous ion beams with the average energy of 30 keV and the current density of 300 μA/cm^2 on the near-surface properties of corundum ceramic.

METHOD OF EXPERIMENT

The object of study is aluminum oxide ceramic (corundum). Samples with the size of 1 cm^2 and the thickness of 0.45–0.50 mm were cut out of standard polished ceramic substrates of 40 × 60 mm^2. Samples were irradiated using an ILM-1 ion implanter equipped with an Pulsar-1M ion source based on a low-pressure glow discharge with a cold hollow cathode [35]. This source provides cylindrical ion beams with the cross-sectional area of about 100 cm^2 with a constant ion current density in this region j of 50 to 500 μA/cm^2 under accelerating voltages U of 5 to 40 keV. The irradiation was performed with argon ions with the energy of 30 keV and the ion current density j = 300 μA/cm^2. Two irradiation modes with continuous beams with the fluences of 10^{16} cm^{-2} (mode A) and 10^{17} cm^{-2} (mode B) were implemented for 6 and 54 s, respectively. The polished surface of ceramic samples was subjected to irradiation.

The temperature of samples during the ion treatments was controlled in an automatic mode using a computer system for measuring digital signals on the basis of ADAM-4000 modules according to the EMF readings of a chromel–alumel thermocouple welded to a blank sample made of stainless steel with the thickness of 1 mm and the area of 1 cm^2. The temperatures of heating of the blank sample at the final phase of the modes A and B were 390 and 1033 K, respectively. The measurement error was ±5 K.

The surface of the irradiated ceramic was analyzed by scanning electron microscopy using a Hitachi TM-3000 instrument equipped with a backscattered electron detector. The static electrical conductivity of ceramic samples was measured in the temperature range T = 25–300°C by the two-probe method of spreading resistance [36].

X-ray phase analysis was performed using an ARL X'tra X-ray diffractometer with a semiconductor Si(Li) Peltier detector (monochromatic CuK_α radiation in the 2θ angle range of 20°–75°). The X-ray pictures were processed using the Powder Cell 2.4 software.

The projective range of Ar^+ ions under the energy of 30 keV in the ceramic was calculated using the KB-03 software program specially developed in a laboratory at the Institute of Electrophysics, Ural Branch, Russian Academy of Sciences (Yekaterinburg, Russia). The software is designed for the calculation of alloying profiles and electron and nuclear energy losses along the target depth under braking of ions on the basis of solving the kinetic Boltzmann equations. The software was developed using the data from [37]. In addition, the projective range of ions was evaluated by the Monte Carlo method (TRIM) [38].

The mechanical properties of the corundum ceramic before and after the radiation treatment were studied by dynamic nanoindentation using a Nano Indenter G 200 nanohardnes tester, which provides indentation in a wide range of loads. A modified Berkovich pyramid (α = 65.27°) was used as an indenter; the load was 250 mN (25 g). About 8–10 indentations were made on the surfaces of samples. The distance between indentations was 50 μm. The statistical measurement error was within 10%.

EXPERIMENTAL RESULTS AND DISCUSSION

In Fig. 1, photomicrographs of the surface of the corundum ceramic sample before and after the ion treatment are shown. It can be seen from Fig. 1a that the sample surface in the initial state was a polished surface, on which one can notice a slight manifestation of granular microstructure and pores distributed randomly over the surface.

It was established that the impact of a continuous beam of argon Ar^+ ions in mode A on the surface of aluminum oxide ceramic does not change the structure of the sample with respect to the initial state. After the irradiation of the surface of the sample in mode B, a clear manifestation of granular microstructure can

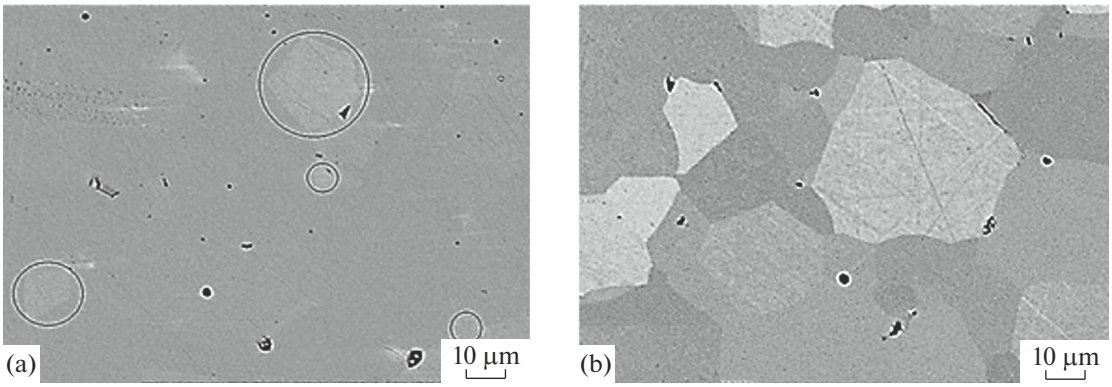

Fig. 1. Surface of ceramic: (a) in the initial state; (b) after ion treatment (mode B).

be seen (Fig. 1b). Thus, the ion treatment in modes A and B does not lead to structural changes in the near-surface layers of the ceramic but only to the manifestation of the initial granular structure, which can be explained by non-coincidence of etching rates of surface grains and intergrain boundaries.

The static electrical conductivity of modified layers of the ceramic was measured using a V7-21A universal voltmeter under constant voltage $U_{max} = 5$ V supplied to the electrodes. The maximum limit of sensitivity in the measurements was 1×10^{-11} A. During the measurements of electrical conductivity of corundum within the sensitivity range of the used instrument, no electrical conductivity was registered. It is known [16, 39] that the ion treatment of ceramic crystals is accompanied by the increase by several orders of magnitudes in the electrical conductivity of irradiated near-surface layers caused by the disturbance in the stoichiometry with respect to oxygen. For corundum, no noticeable changes in the conductivity were registered, which is explained by preservation of the initial stoichiometric composition.

In Fig. 2, the *P*–*h* diagram of the kinetic indentation of the corundum ceramic in the initial stated before the surface treatment under the maximum load applied on the indenter $P_{max} = 250$ mN is shown. The appearance of the *P*–*h* diagram after the surface treatment does not change. The diagram has the following regions: the loading branch *1* characterizing the resistance of the material to plastic deformations; the horizontal region *2* corresponding to the exposure of the sample under the maximum load; and the region of unloading to the zero value (full unloading) *3* [40, 41]. The presence of these regions corresponds to the recommendations of the hardness measurement standards concerning the sequence of loading the sample [42, 43]. The time of loading and unloading in all cases was the same, namely, 75 s. From Fig. 2, it can be seen that the residual depth h_0 of an indentation after unloading differs significantly from the maximum indenter penetration depth h_{max}. This indicates active processes of material recovery in the deformed region in the unloading mode. The process of change in the indentation size can be evaluated on the basis of the value of elastic deformation of an indentation:

$$\alpha = \frac{(h_{max} - h_0)}{h_{max}}. \quad (1)$$

Under the maximum load on applied on the indenter $P_{max} = 250$ mN, the value of elastic deformation α was 0.47 for the unirradiated ceramic and $\alpha = 0.51$ for the irradiated sample in mode A.

The mechanical characteristics were determined on the basis of the developed curves of the *P*–*h* diagram using the Oliver and Pharr method [44].

In Table 1, the deformation characteristics of the studied ceramic before and after the Ar^+ treatment registered under the maximum load applied on the indenter $P_{max} = 250$ mN are given.

According to the nanoindentation data given in Table 1, after the treatment with the Ar^+ ion beam, there is a change in the mechanical properties of near-surface layers of the corundum ceramic, namely, the

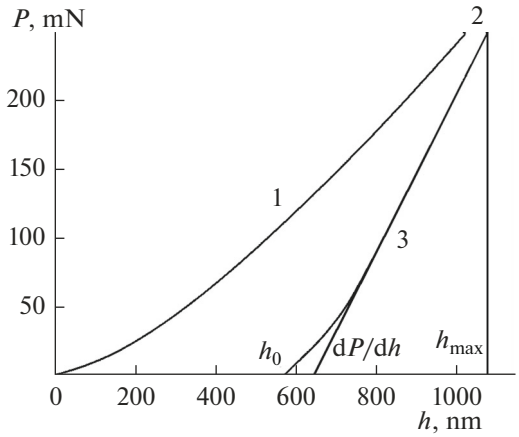

Fig. 2. *P*–*h* indentation diagram for ceramic before ion treatment with the load on indenter $P_{max} = 250$ mN.

Table 1. Mechanical properties of corundum ceramic before and after Ar^+ treatment

Properties	Radiation		
	without radiation	mode A	mode B
Nanohardness, H_{IT}, GPa	14.8 ± 0.67	24.5 ± 2.53	22.7 ± 1.18
Modulus of elasticity (Young's modulus), E_{IT}, GPa	188.3 ± 4.17	429.6 ± 19.4	378.2 ± 15.6
Maximum indenter penetration depth, h_{max}, nm	1071.2 ± 16.4	807 ± 30.8	840 ± 10.6
H_{IT}^3 / E_{IT}^2, GPa	0.09	0.08	0.08

Table 2. The projective ranges of Ar^+ ions

Ranges of ions, nm	Calculation method	
	software [37]	Monte Carlo (TRIM) [38]
Average projective range, R_p, nm	18.8	15.9
Mean-square variance of projective ranges, ΔR_p, nm	7.3	3.8
Mean-square variance of transverse ranges, $R_{p\perp}$, nm	5.7	3.0

increase in the modulus of elasticity by about 2 times and the increase in the nanohardness by 1.5 times compared to the initial values. The maximum indenter penetration depth after the treatment decreases by about $\Delta h_{max} = 248 \pm 20.4$ nm. The change in the deformation characteristics after the irradiation with continuous beams using different fluences is ambiguous. The observed slight decrease in the H_{IT} and E_{IT} values in mode B compared to mode A can be explained by two simultaneous processes caused by the radiation impact. Along with the ion implantation, there is etching of thin near-surface layers under the ion treatment. Prevalence of the latter process over the former one with the increase in the fluence can eventually lead to the decrease in the modification efficiency. Note that, after the irradiation of the ceramic in modes A and B, the nanoindentation results lie within the mean-square deviation range of measurements (Table 1).

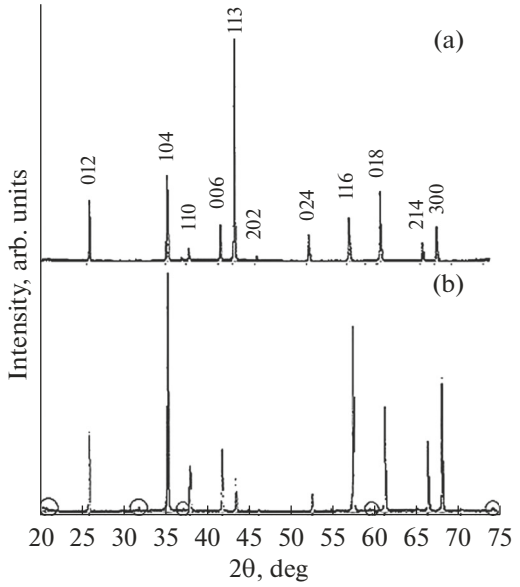

Fig. 3. Diffraction patterns: (a) initial corundum ceramic, (b) after ion treatment (mode B).

The resistance of material to plastic deformation according to [45] is evaluated according to the value of the parameter $K = H_{IT}^3 / E_{IT}^2$. After the ion treatment, the value of this parameter decreases (Table 1), thus indicating the increase in the plasticity of modified ceramic layers.

In Table 2, the results of the calculations of projective ranges of Ar+ ions using the algorithms presented in [37, 38] are demonstrated.

From the comparison of the results in Tables 1 and 2, it can be seen that the observed change in the deformation properties occurs at depths h_{max} which significantly exceed the depth R_p of the radiation penetration of implanted ions. This can be explained by the long-range effect model observed in different materials under beam impacts [46–48].

To determine the reasons that are responsible for the change in the deformation characteristics of the modified ceramic surface, the structural-phase analysis of near-surface layers was performed. The results of this analysis are given in Fig. 3. The analysis of the results using the Powder Cell 2.4 software shows that, in the initial state and after the radiation impact, the ceramic contains only the α-Al_2O_3 phase characterized by trigonal syngony.

In the X-ray picture after the irradiation (Fig. 3b), along with corundum, additional reflexes typical of the phase can be clearly seen. The same phase is pres-

Table 3. Results of X-ray diffraction analysis of corundum ceramic samples before and after the Ar^+ treatment

Characteristics	Without radiation	Radiation	
		Mode A	Mode B
Coherent scattering region size L, nm	195	119	103
Crystal lattice microstrains, $\Delta d/d$	0.2×10^{-3}	0.3×10^{-3}	0.4×10^{-3}

ent in the initial state; because of lower intensity; the peaks are not so clearly seen (Fig. 3a). It is impossible to analyze the presence of the unknown phase because of the precise composition of substrate material used in the study is unknown.

As can be seen from the diffraction patterns shown in Fig. 3, the ion treatment of the corundum surface leads to the change in the intensities of the reflexes. This can be explained by the manifestation of the dislocation mechanism under the action of the ion treatment [15], which leads to strengthening or weakening of reflections of X-ray beams from plane systems. In Table 3, the results of the X-ray structural analysis are shown.

According to the X-ray structural studies, the size (L) of the coherent scattering region of the α phase of corundum and the crystal lattice microstrains ($\Delta d/d$) were evaluated (Table 3). In the ceramic layer modified with a continuous Ar^+ ion beam, the L value was lower than in the initial state. The irradiation increased the ($\Delta d/d$) value. The cumulative experimental results confirm the assumption about the manifestation of the dislocation strengthening mechanism.

Hence, the modification of the near-surface layers of the ceramic under the action of a continuous Ar+ ion beam is of a purely radiation nature and can be explained within the shock wave mechanism model typical of metals and alloys [11, 46–48].

CONCLUSIONS

The effect of continuous Ar^+ ion beams with energy of 30 keV and fluences of 10^{16} and 10^{17} cm^{-2} at the ion current density of 300 $\mu A/cm^2$ on aluminum oxide ceramic (corundum) was studied.

The radiation treatment does not lead to structural changes of the ceramic in near-surface layers; only the initial granular structure is shown owing to the difference in the etching rates of surface grains and intergrain boundaries.

In the irradiated ceramic, no noticeable change in the electrical conductivity typical of ion crystals under ion irradiation is observed [39]. This means that, in aluminum oxide ceramic, in the process of ion treatment, disturbance in the stoichiometry with respect to oxygen is insignificant and its dielectric properties change only slightly.

The ion treatment does not lead to change in the phase composition. Simultaneously, a partial rotation of planes is observed, which is manifested by the change in the intensity of X-ray reflexes. The increase in the fluence causes the decrease in the coherent scattering region and the increase in the crystal lattice microstrains.

After the irradiation of the ceramic with Ar^+ ions, the mechanical properties of the near-surface layers change, which is manifested by the increase in both hardness and modulus of elasticity of the modified surface. Simultaneously, a long-range effect is observed: the mechanical properties change at a depth significantly exceeding the radiation penetration depth of implanted ions.

ACKNOWLEDGMENTS

This work was supported by the Russian Science Foundation, project no. 17-19-01082.

REFERENCES

1. Grishunin, V.A., Gromov, V.E., Ivanov, Yu.F., Teresov, A.D., and Konovalov, S.V., Evolution of the phase composition and defect substructure of rail steel subjected to high intensity electron-beam treatment, *J. Surf. Invest.*, 2013, vol. 5, pp. 990–995.
2. Surzhikov, A.P., Frangulyan, T.S., Ghyngazov, S.A., and Koval, N.N., Structural-phase transformations in nearsurface layers of alumina-zirconium ceramics induced by low-energy high-current electron beams, *Nucl. Instrum. Methods Phys. Res., Sect. B*, 2009, vol. 7, pp. 1072–1076.
3. Gromov, V.E., Gorbunov, S.V., Ivanov, Y.F., Vorobiev, S.V., and Konovalov, S.V., Formation of surface gradient structural-phase states under electron-beam treatment of stainless steel, *J. Surf. Invest.*, 2011, vol. 5, pp. 974–978.
4. Ivanov, Y., Alsaraeva, K., Gromov, V., Konovalov, S., and Semina, O., Evolution of Al-19.4Si alloy surface structure after electron beam treatment and high cycle fatigue, *Mater. Sci. Technol.*, 2015, vol. 13, pp. 1523–1529.
5. Šugár, P., Frnčiík, M., Šugárová, J., and Sahul, M., Laser beam milling of alumina ceramics—the impact on material removal efficiency and machined surface morphology, *Solid State Phenom.*, 2017, vol. 261, pp. 143–150.
6. Savruk, E.V. and Smirnov, S.V., Analysis of the alumina ceramics structure after electron and laser treatment, *Zavod. Lab., Diagn. Mater.,* 2011, no. 6, pp. 32–35.
7. Renk, T.J., Provencio, P.P., Prasad, S.V., Shlapakovski, S.S., Petrov, A., Yatsui, A., Kiyoshi, J., and

Weihua, S.H., Materials modification using intense ion beams, *Proc. IEEE,* 2004, vol. 7, pp. 1057–1081.

8. Maslyaev, S.A., Morozov, E.V., Romakhin, P.A., Pimenov, V.N., Gribkov, V.A., Tikhonov, A.N., Bondarenko, G.G., Dubrovsky, A.V., Kazilin, E.E., Sasinovskaya, I.P., and Sinitsyna, O.V., Damage of Al_2O_3 ceramics under the action of pulsed ion and plasma fluxes and laser irradiation, *Inorg. Mater.: Appl. Res.*, 2016, vol. 7, no. 3, pp. 330–339.
9. Ivanov, L.I., Pimenov, V.N., and Gribkov, V.A., Interaction of power pulsed fluxes of energy with materials, *Fiz. Khim. Obrab. Mater.*, 2008, no. 1, pp. 23–37.
10. Schmidt, B. and Wetzig, K., *Ion Beams in Materials Processing and Analysis*, New York: Springer Verlag, 2013.
11. Ovchinnikov, V.V., Makhin'ko, F.F., and Solomonov, V.I., Thermal-spikes temperature measurement in pure metals under argon ion irradiation (E = 5–15 keV), *J. Phys.: Conf. Ser.*, 2015, vol. 652, pp. 1–8.
12. Elke, W. and Werner, W., *Ion Beam Modification of Solids,* Springer Series in Surface Sciences, New York: Springer-Verlag, 2016.
13. Zatsepin, D.A., Cholakh, S.O., and Vainshtein, I.A., *Ionnaya modifikatsiya funktsional'nykh materialov* (Ion Modification of Functional Materials), Yekaterinburg: Ural. Fed. Univ., 2014.
14. Romanov, I.G. and Tsareva, I.N., High-power pulsed ion beam modification of the surface properties of alumina ceramics, *Tech. Phys. Lett.*, 2001, vol. 27, no. 8, pp. 695–697.
15. Ghyngazov, S.A., Vasil'ev, I.P., Surzhikov, A.P., Frangulyan, T.S., and Chernyavskii, A.V., Ion processing of zirconium ceramics by high-power pulsed beams, *Tech. Phys.*, 2015, vol. 60, no. 1, pp. 128–132.
16. Kostenko, V., Pavlov, S., and Nikolaeva, S., Influence of a high-power pulsed ion beam on the mechanical properties of corundum ceramics, *IOP Conf. Ser.: Mater. Sci. Eng.*, 2018, vol. 289, pp. 1–7.
17. Fedorov, D.G. and Seleznev, B.I., Formation of structures of Schottky diodes on GaN with the use of ion implantation, *Elektron. Mirkoelektron. SVCh,* 2016, no. 1, pp. 190–192.
18. Aleksandrov, P.A., Demakov, K.D., Shemardov, S.G., and Belova, N.E., Application of ion implantation for the modification of silicon-on-sapphire epitaxial systems, their structure, and properties, *J. Surf. Invest.: X-ray, Synchrotron Neutron Tech.,* 2017, vol. 11, no. 4, pp. 790–800.
19. Anderson, J.T., Greenlee, J., Feigelson, B., Hite, J., Kub, J.F., and Hobart, K., Improved vertical GaN Schottky diodes with ion implanted junction termination extension, *ECS J. Solid State Sci. Technol.*, 2016, vol. 5, pp. 176–178.
20. Sikharulidze, G.G., Generation of an ion beam in a glow-discharge source, *Instrum. Exp. Tech.*, 2009, vol. 52, no. 2, pp. 249–252.
21. Nakhlestkin, A.A. and Arkhireev, A.G., Ion accelerators, *Materialy I Mezhdunarodnoi molodezhnoi nauchnoi konferentsii "Molodezh' v nauke: Novye argumenty," g. Lipetsk, Rossiya, 25 dekabrya 2014 g.* (Proc. I Int. Youth Sci. Conf. "Youth in Science: New Arguments," Lipetsk, Russia, December 25, 2014), Gorbenko, A.V., Ed., Lipetsk: Argument, 2015, part 1, pp. 14–16.
22. Frolova, V.P., Generation of high-charge bismuth ions in a vacuum-spark ion source, *Elektron. Sredstva Sist. Uprav.,* 2015, no. 1, pp. 230–233.
23. Goncharov, L.A. and Grigor'yan, V.G., Ion sources for ion-beam technology operations, *Prikl. Fiz.*, 2007, no. 5, pp. 67–70.
24. Ryabchikov, A.I., Accelerators of charged particles SINP radiant units and their use in science and technology, *Izv. Tomsk. Politekh. Univ.*, 2000, no. 1, pp. 17–43.
25. Vlasov, I., Panin, S., Sergeev, V.P., Naidfeld, V., Kalashnikov, M.P., Bogdanov, O., and Ovechkin, B., Zr^+ ion-beam surface treatment of $30CrMnSiNi_2$ steel for improving its fatigue durability, *Adv. Mater. Res.*, 2014, vol. 872, pp. 219–224.
26. Demin, A.S., Morozov, E.V., Maslyaev, S.A., Pimenov, V.N., Gribkov, V.A., Demina, E.V., Sasinovskaya, I.P., Sirotinkin, V.P., Sprygin, U.S., Bondarenko, G.G., Tikhonov, A.N., and Gaidar, A.I., The influence of a powerful stream of deuterium ions and deuterium plasma on the structural state of the surface layer of titanium, *Inorg. Mater.: Appl. Res.*, 2017, vol. 8, no. 3, pp. 412–418.
27. Uglov, V.V., Remnev, G.E., Kuleshov, A.K., and Saltymakov, M.S., Modification of (Ti,Cr)N coatings on a hard alloy under the action of high-power pulsed ion beams, *Inorg. Mater.: Appl. Res.*, 2011, vol. 2, no. 3, pp. 242–246.
28. Zlobin, V.N., Vasil'ev, I.P., and Zelyakovskii, D.V., Use of ion implantation in engine engineering, *Fundam. Issled.,* 2015, no. 7-4, pp. 707–711.
29. Zhong, H., Zhang, J., Shen, J., Yu, X., Liang, G., Cui, X., Zhang, X., Zhang, G., Yan, S., and Le, X., Craters forming mechanism of high speed steel irradiated by intense pulsed ion beam, *Nucl. Instrum. Methods Phys. Res., Sect. B,* 2017, vol. 409, pp. 298–301.
30. Kurzina, I.A., Kozlov, E.V., Popova, N.A., Kalashnikov, M.P., Nikonenko, E.L., Savkin, K.P., Oks, E.M., and Sharkeev, Yu.P., Modifying the structural phase state of fine-grained titanium under conditions of ion irradiation, *Bull. Russ. Acad. Sci.: Phys.*, 2012, vol. 76, no. 11, pp. 1238–1245.
31. Konnov, A.G., Kukarenko, V.A., Belyi, A.V., and Sharkeev, Yu.P., Ion-modified submicrocrystalline titanium and zirconium alloys for medicine and engineering, *Mekh. Mash., Mekh., Mater.*, 2013, no. 22, pp. 47–53.
32. Novoselov, A.A. and Bayankin, V.Ya., Segregation as manifestation of long-range effect occurring at ion implantation of rolled CuNi foils, *Vestn. Permsk. Univ., Ser.: Fiz.,* 2013, no. 3, pp. 60–67.
33. Danelyan, L.S., Korshunov, S.N., Mansurova, A.N., Zatekin, V.V., Kulikauskas, V.S., Borovitskaya, I.V., Paramonova, V.V., and Lyakhovitskyi, M.M., Effect of dose and energy of Ar^+ ions on the surface properties of vanadium and its alloys, *J. Surf. Invest.: X-ray, Synchrotron Neutron Tech.*, 2014, vol. 8, no. 2, pp. 216–219.
34. Shushkov, A.A., Vorob'ev, V.L., Vakhrushev, A.B., Bykov, P.V., and Bayankin, V.Ya., Mechanical properties of carbon steel ST3 irradiated by argon ions with different ion current densities, *Khim. Fiz. Mezoskopiya*, 2012, no. 14, pp. 97–105.
35. Gavrilov, N.V., Mesyats, G.A., Nikulin, S.P., Radkovskii, G.V., Eklind, A., Perry, A.J., and Treglio, J.R.,

New broad beam gas ion source for industrial application, *J. Vac. Sci. Technol.*, 1996, vol. 14, pp. 1050–1055.

36. Miroshkin, V.P., Panova, Ya.I., and Pasynkov, V.V., Dielectric relaxation in polycrystalline ferrites, *Phys. Solid State,* 1981, vol. 66, pp. 779–782.
37. Burenkov, A.F., Komarov, F.F., Kumakhov, M.A., and Temkin, M.M., *Prostranstvennye raspredeleniya energii, vydelennoi v kaskade atomnykh stolknovenii v tverdykh telakh* (Spatial Distribution of Energy Released in the Cascade of Atomic Collisions in Solids), Moscow: Energoizdat, 1985.
38. Biersack, J.P. and Haggmark, L.G., A Monte Carlo computer program for the transport of energetic ions in amorphous targets, *Nucl. Instrum. Methods*, 1980, vol. 174, pp. 257–269.
39. Pichugin, V.F., Frangul'yan, T.S., Kul'kov, S.N., et al., Zirconium dioxide electric conductivity and its variation under ion irradiation, *Fiz. Khim. Obrab. Mater.,* 1996, no. 6, pp. 17–22.
40. Golovin, Yu.I., *Vvedenie v nanotekhniku* (Introduction into Nanoengineering), Moscow: Mashinostroenie, 2007.
41. Kolmakov, A.G., Terent'ev, V.F., and Bakirov, M.B., *Metody izmereniya tverdosti* (Measurements of Solidity), Moscow: Intermet Inzhiniring, 2005.
42. *ISO 14577-4:2016: Metallic Materials, Instrumented Indentation Test for Hardness and Materials Parameters, Part 4: Test Method for Metallic and Non-Metallic Coatings,* Geneva: Int. Org. Standart., 2016.
43. Moshchenok, V.I., *Novye metody opredeleniya tverdosti materialov: monografiya* (New Methods for Determination of Solidity of Materials: Monograph), Kharkov: Khar'k. Nats. Avtom.-Dorozhn. Univ., 2013.
44. Oliver, W.C. and Pharr, G.M., Measurement of hardness and elastic modulus by instrumented indention: Advanced in understanding and refinements to methodology, *J. Mater. Res.*, 2004, vol. 19, no. 1, pp. 3–20.
45. Leyland, A. and Matthews, A., On the significance of the H/E ratio in wear control: a nanocomposite coating approach to optimized tribological behavior, *Wear*, 2000, vols. 1–2, pp. 1–11.
46. Tereshkov, I.V., Abidzina, V.V., Elkin, I.E., Tereshkov, A.M., Glushchenko, V.V., and Stoye, S., The formation of nanoclusters in metals by the low-energy ion irradiation, *Surf. Coat. Technol.*, 2007, vol. 201, pp. 8552–8556.
47. Stepanov, V.A. and Khmelevskaya, V.S., Radiation-induced plastic deformation and the long-range action effect, *Tech. Phys.,* 2011, vol. 56, no. 9, pp. 1272–1276.
48. Aparina, N.P., Guseva, M.I., Kolbasov, B.N., Korshunov, S.N., Mansurova, A.N., and Martynenko, Yu.V., Some aspects of the long-range effect, *Vopr. At. Nauki Tekh., Ser.: Termoyad. Sint.*, 2007, no. 3, pp. 18–27.

Translated by E. Petrova